

Conversion of Benzaldehyde Imines into Isocyanides at a Low-Valent Molybdenum Center. Preparation and Reactivities of Isocyanide–Dinitrogen Complexes *trans*-[Mo(RNC)(N₂)(Ph₂PCH₂CH₂PPh₂)₂] (R = Aryl, Alkyl)¹

Hidetake Seino,^{2a} Chirima Arita,^{2a} Daigo Nonokawa,^{2a} Goh Nakamura,^{2a,b}
Yuji Harada,^{2a,b} Yasushi Mizobe,^{*,2a,c} and Masanobu Hidai^{*,2b}

Institute of Industrial Science, The University of Tokyo, Roppongi, Minato-ku, Tokyo 106-8558, Japan, Department of Chemistry and Biotechnology, Graduate School of Engineering, The University of Tokyo, Hongo, Tokyo 113-8656, Japan, and Institute for Molecular Science, Myodaiji, Okazaki 444-8585, Japan

Received June 14, 1999

The molybdenum dinitrogen complex *trans*-[Mo(N₂)₂(dppe)₂] (**1**; dppe = Ph₂PCH₂CH₂PPh₂) reacts with benzaldehyde imines PhCH=NR (R = Ph, C₆H₄Me-*p*, C₆H₄OMe-*p*, C₆H₄F-*p*, C₆H₄NMe₂-*p*, Buⁿ, Prⁱ, CH₂Ph) in benzene at reflux to give a series of isocyanide–dinitrogen complexes *trans*-[Mo(RNC)(N₂)(dppe)₂] (**7**) with the concurrent formation of benzene. The structure of **7a** (R = Ph) has been determined by X-ray crystallography. Treatment of **7a** and **7f** (R = Buⁿ) with CO (1 atm) or *p*-MeOC₆H₄CN results in the replacement of the coordinated N₂ by these ligands, affording *trans*-[Mo(RNC)(L)(dppe)₂] (L = CO (**9**), *p*-MeOC₆H₄CN (**10**)). The complex containing two different isocyanides *trans*-[Mo(PhNC)-(BuⁿNC)(dppe)₂] was obtained analogously from **7a** and BuⁿNC. On the other hand, when benzene or toluene solutions of **7a** and **7e** (R = C₆H₄NMe₂-*p*) were first heated under Ar up to 80–90 °C for a short period to dissociate the coordinated N₂ and then treated with H₂ at room temperature, dihydrogen complexes *trans*-[Mo(RNC)(η²-H₂)(dppe)₂] (**13**) were produced. The X-ray analyses have revealed the detailed structures for **9a** (R = Ph), **10a** (R = Ph), and **13e** (R = C₆H₄NMe₂-*p*) along with the bis(isocyanide) complex *trans*-[Mo(PhNC)₂(dppe)₂].

Introduction

Since the isolation of the first Mo dinitrogen complex *trans*-[Mo(N₂)₂(dppe)₂] (**1**; dppe = Ph₂PCH₂CH₂PPh₂) in this laboratory,³ intensive efforts have been devoted to investigate reactivities of the N₂ ligand in **1** and related Mo and W complexes such as *trans*-[W(N₂)₂(dppe)₂] (**2**) and *cis*-[M(N₂)₂(PMe₂Ph)₄] (M = Mo, W), aiming at development of a new type of N₂-fixing systems.⁴ Now it has become apparent that these Mo and W dinitrogen complexes are distinctive from other numerous N₂ complexes hitherto reported in the reactivity of the coordinated N₂ which gives rise to the formation of nitrogenous ligands and compounds under ambient conditions.^{4,5}

One of the other intriguing reactions promoted by **1** is the decarbonylation of various oxygen-containing

organic compounds including aldehydes, formamides, carboxylic acid esters, and alcohols,⁶ where **1** serves as a versatile precursor to generate a highly reactive, coordinatively unsaturated species by dissociating the N₂ ligands. Reactions of this type are exemplified by the formation of *trans*-[Mo(CO)(DMF)(dppe)₂] (**3**; DMF = *N,N*-dimethylformamide) upon treatment of **1** with an excess of DMF in benzene at reflux.⁷ Interestingly, the DMF ligand in **3** is so labile that **3** is readily converted to *trans*-[Mo(CO)(N₂)(dppe)₂] (**4**) and [Mo(CO)(dppe)₂] (**5**).^{6a} From these carbonyl complexes as well as their W analogues derived similarly from **2**, a number of carbonyl complexes of the types [M(CO)(L)(dppe)₂] (M = Mo, L = Lewis bases, nitrile, olefin,^{6a,8} H₂,⁹ hydrosilanes;¹⁰ M = Mo, W; L = vinylidene¹¹) and [M(CO)H-

(1) Preparation and Properties of Molybdenum and Tungsten Dinitrogen Complexes. 64. Part 63: see ref 15.

(2) (a) Institute of Industrial Science. (b) Department of Chemistry and Biotechnology. (c) Institute for Molecular Science.

(3) (a) Hidai, M.; Tominari, K.; Uchida, Y.; Misono, A. *J. Chem. Soc., Chem. Commun.* **1969**, 1392. (b) Hidai, M.; Tominari, K.; Uchida, Y. *J. Am. Chem. Soc.* **1972**, 94, 110.

(4) (a) Hidai, M.; Mizobe, Y. *Chem. Rev.* **1995**, 95, 1115. (b) Hidai, M.; Ishii, Y. *Bull. Chem. Soc. Jpn.* **1996**, 69, 819.

(5) (a) Richards, R. L. *Coord. Chem. Rev.* **1996**, 154, 83. (b) Bazhenova, T. A.; Shilov, A. E. *Coord. Chem. Rev.* **1995**, 144, 69. (c) Gambarotta, S. *J. Organomet. Chem.* **1995**, 500, 117. (d) Leigh, G. J. *Acc. Chem. Res.* **1992**, 25, 177.

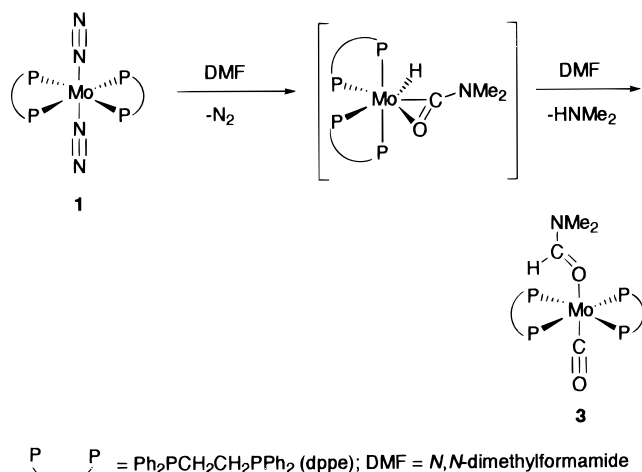
(6) (a) Sato, M.; Tatsumi, T.; Kodama, T.; Hidai, M.; Uchida, T.; Uchida, Y. *J. Am. Chem. Soc.* **1978**, 100, 4447. (b) Tatsumi, T.; Tominaga, H.; Hidai, M.; Uchida, Y. *J. Organomet. Chem.* **1981**, 215, 67. (c) Tatsumi, T.; Tominaga, H.; Hidai, M.; Uchida, Y. *J. Organomet. Chem.* **1981**, 218, 177.

(7) Mizobe, Y.; Ishida, T.; Egawa, Y.; Ochi, K.; Tanase, T.; Hidai, M. *J. Coord. Chem.* **1991**, 23, 57.

(8) Tatsumi, T.; Tominaga, H.; Hidai, M.; Uchida, Y. *J. Organomet. Chem.* **1980**, 199, 63.

(9) (a) Kubas, G. J.; Ryan, R. R.; Wroblewski, D. A. *J. Am. Chem. Soc.* **1986**, 108, 1339. (b) Kubas, G. J.; Burns, C. J.; Eckert, J.; Johnson, S. W.; Larson, A. C.; Vergamini, P. J.; Unkefer, C. J.; Khalsa, G. R. K.; Jackson, S. A.; Eisenstein, O. *J. Am. Chem. Soc.* **1993**, 115, 569.

Scheme 1



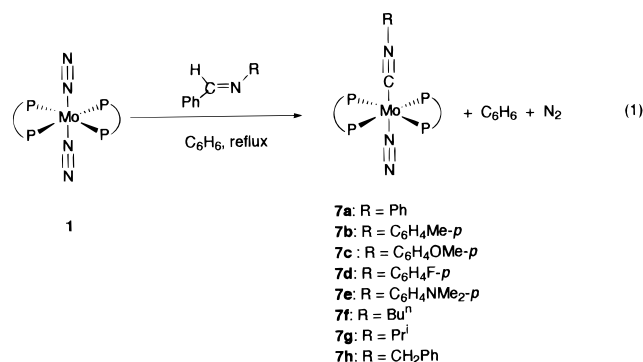
(X)(dppe)₂] (M = Mo, W; X = alkynyl;¹¹ M = W, X = carbonate, carbamate,¹² hydride¹³) have been prepared.

The mechanism for the formation of **3** from **1** involves the cleavage of the aldehydic C–H bond in DMF at the coordinatively unsaturated Mo center to give a hydrido-carbamoyl species followed by the elimination of dimethylamine (Scheme 1). This has been verified by the isolation of [WH(η²-CONMe₂)(dppe)₂] (**6**) from the reaction of **2** with DMF under controlled conditions. As expected, when heated in benzene in the presence of DMF, **6** is converted to *trans*-[W(CO)(DMF)(dppe)₂] with concurrent formation of HNMe₂.¹³

Now the study has been extended to the reactions of **1** with benzaldehyde imines PhCH=NR (R = aryl, alkyl) instead of aldehydic compounds, and we have found that unprecedented conversion of the imines into isocyanides takes place at the Mo center to give a series of isocyanide–dinitrogen complexes *trans*-[Mo(RNC)(N₂)(dppe)₂] (**7**). In this paper, details of the syntheses and characterization of **7** are described, together with the reactivities of **7** toward a series of neutral ligands including CO, nitriles, isocyanides, and H₂. A part of this work has been reported recently as a communication.¹⁴

Results and Discussion

Preparation of Isocyanide–Dinitrogen Complexes 7. When reacted with a range of PhCH=NR in benzene at reflux for 2 h, the dinitrogen complex **1** afforded **7** in moderate yields (eq 1). Employment of the



imines with R = C₆H₄X-*p* (X = H, Me, OMe, F, NMe₂), Buⁿ, Prⁱ, and CH₂Ph gave the well-defined complexes

7; however, use of the imines having the substituents C₆H₄X-*p* (X = CF₃, COOEt) and Bu^t for R did not afford the corresponding compounds. Due to the thermal instability, **7h** (R = CH₂Ph) once produced proved to decompose rapidly under the conditions employed. Thus, **7h** was obtained in satisfactory yield by refluxing the reaction mixture for only 5 min. The conversion of imines at the Mo center into the corresponding isocyanides appears to proceed via the scission of both the C–Ph and C–H bonds on the benzylidene carbon. This was confirmed by the concurrent formation of benzene with **7a** and **7b** in the reaction of **1** with PhCH=NR or PhCH=NC₆H₄Me-*p* (0.71 and 0.73 mol of C₆H₆/mol of **1**, respectively).

Although the reactions of several aliphatic aldehyde imines R'CH=NR (R = alkyl, aryl; R' = alkyl) with **1** were attempted, complexes containing the RNC ligand were not produced. Interestingly, from the reaction mixtures of **1** with the imines that remained intact under these conditions, a Mo(0) complex with a novel tetradentate phosphine [Mo(η⁶-C₆H₄(PPhCH₂CH₂PPh₂)₂)-(dppe)] has been isolated in low yield. Characterization and the improved method for preparation of this complex from **1** by thermolysis have already been reported separately.¹⁵ It is to be noted that the reactions of **1** with various isocyanides give bis(isocyanide) complexes *trans*-[Mo(RNC)₂(dppe)₂] (R = alkyl, aryl) exclusively, and the formation of the monosubstituted complexes **7** was not observed.¹⁶

To our knowledge, little is known about the direct transformation of imines into isocyanides. In contrast, insertion of isocyanides into M–R bonds leading to η¹- or η²-iminoacyls is a well-precedented process.¹⁷ For certain metal iminoacyl species, formation of imines by successive alkyl migration onto the iminoacyl carbon is also known.¹⁸ The novel conversion of benzylidene-anilines into isocyanides reported here might proceed by following these processes in the reverse direction (Scheme 2). Thus, oxidative addition of the benzylidene C–H bond occurs initially at the coordinatively unsaturated Mo(0) center generated by thermolysis of **1**, giving a hydrido–iminoacyl intermediate [MoH{C(=NR)Ph}](dppe)₂. Deinsertion of RNC from the iminoacyl ligand and the following reductive elimination of ben-

(10) (a) Luo, X.-L.; Kubas, G. J.; Bryan, J. C.; Burns, C. J.; Unkefer, C. J. *J. Am. Chem. Soc.* **1994**, *116*, 10312. (b) Luo, X.-L.; Kubas, G. J.; Burns, C. J.; Bryan, J. C.; Unkefer, C. J. *J. Am. Chem. Soc.* **1995**, *117*, 1159.

(11) Nakamura, G.; Harada, Y.; Mizobe, Y.; Hidai, M. *Bull. Chem. Soc. Jpn.* **1996**, *69*, 3305.

(12) Ishida, T.; Hayashi, T.; Mizobe, Y.; Hidai, M. *Inorg. Chem.* **1992**, *31*, 4481.

(13) Ishida, T.; Mizobe, Y.; Tanase, T.; Hidai, M. *J. Organomet. Chem.* **1991**, *409*, 355.

(14) Nakamura, G.; Harada, Y.; Arita, C.; Seino, H.; Mizobe, Y.; Hidai, M. *Organometallics* **1998**, *17*, 1010.

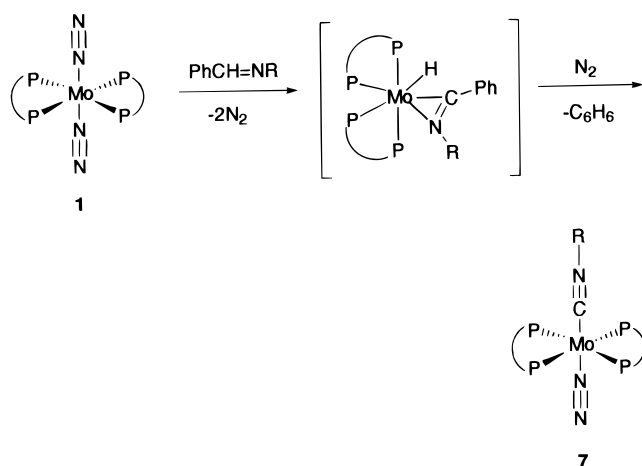
(15) Arita, C.; Seino, H.; Mizobe, Y.; Hidai, M. *Chem. Lett.* **1999**, 611.

(16) (a) Chatt, J.; Elson, C. M.; Pombeiro, A. J. L.; Richards, R. L.; Royston, G. H. D. *J. Chem. Soc., Dalton Trans.* **1978**, 165. (b) Pombeiro, A. J. L.; Pickett, C. J.; Richards, R. L.; Sangokoya, S. A. *J. Organomet. Chem.* **1980**, *202*, C15. (c) Pombeiro, A. J. L.; Richards, R. L. *Coord. Chem. Rev.* **1990**, *104*, 13.

(17) Durfee, L. D.; Rothwell, I. P. *Chem. Rev.* **1988**, *88*, 1059.

(18) (a) Durfee, L. D.; Fanwick, P. E.; Rothwell, I. P.; Folting, K.; Huffman, J. C. *J. Am. Chem. Soc.* **1987**, *109*, 4720. (b) Koschmieder, S. U.; Hussain-Bates, B.; Hursthouse, M. B.; Wilkinson, G. *J. Chem. Soc., Dalton Trans.* **1991**, 2785. (c) Lai, R.; Desbois, O.; Zamkotsian, F.; Faure, R.; Feneau-Dupont, J.; Declercq, J.-P. *Organometallics* **1995**, *14*, 2145. (d) Cámpora, J.; Buchwald, S. L.; Gutiérrez-Puebla, E.; Monge, A. *Organometallics* **1995**, *14*, 2039.

Scheme 2



zene affords $[\text{Mo}(\text{CNR})(\text{dppe})_2]$ (**8**), which rapidly binds N_2 to yield **7**. Many attempts to isolate or detect **8** were carried out, but failed.

Since the hydrido-carbamoyl intermediate **6** was able to be isolated only for W in the related decarbonylation reaction of DMF (Scheme 1), W complex **2** was allowed to react with benzaldehyde imines under the analogous conditions. However, neither the isocyanide-dinitrogen complexes nor the hydrido-iminoacyl complexes were obtained.

Since a variety of benzaldehyde imines are readily available, the reactions reported here are attractive as a route to isocyanides. However, the reaction proceeded only stoichiometrically, and the liberation of free isocyanides was not observed in the reactions with an excess amount of benzaldehyde imines.

Characterization of 7. The structure of **7a** has been determined in detail by single-crystal X-ray analysis. The ORTEP drawing is shown in Figure 1, while the important bond lengths and angles are listed in Table 1. Complex **7a** has a slightly distorted octahedral structure with mutually trans PhNC and N_2 ligands bound to the Mo center in an end-on fashion. In the PhNC ligand, the $\text{Mo}-\text{C}(1)-\text{N}(1)$ linkage is almost linear ($176.7(3)^\circ$), while the $\text{C}(1)-\text{N}(1)-\text{C}(2)$ bond is slightly bent, with an angle of $167.4(4)^\circ$. The $\text{C}(1)-\text{N}(1)$ bond length at $1.179(4)$ Å is unexceptional for the isocyanide ligand of this coordination mode. With respect to the N_2 ligand, the $\text{Mo}-\text{N}(2)-\text{N}(3)$ linkage is nearly linear ($177.1(3)^\circ$), and the $\text{N}(2)-\text{N}(3)$ distance at $1.102(3)$ Å is comparable to those in free N_2 ($1.0976(2)$ Å)¹⁹ and **4** ($1.09(2)$ Å).^{6a}

Spectroscopic and analytical data for **7a** are in good agreement with the solid-state structure. Thus, the IR spectrum shows two intense bands at 2049 and 1910 cm^{-1} assignable to $\nu(\text{NN})$ of the coordinated N_2 and $\nu(\text{NC})$ of the PhNC ligand, respectively, while the $^{31}\text{P}\{-^1\text{H}\}$ NMR spectrum exhibits one singlet at δ 68.9 due to the two dppe ligands constituting the basal plane of the octahedral structure. The other new complexes **7b–7h** show the analogous spectral features, indicating that the structures are essentially identical.²⁰

Now a series of the N_2 complexes of the type $\text{trans}[\text{Mo}(\text{L})(\text{N}_2)(\text{dppe})_2]$ are available, where the ligand L

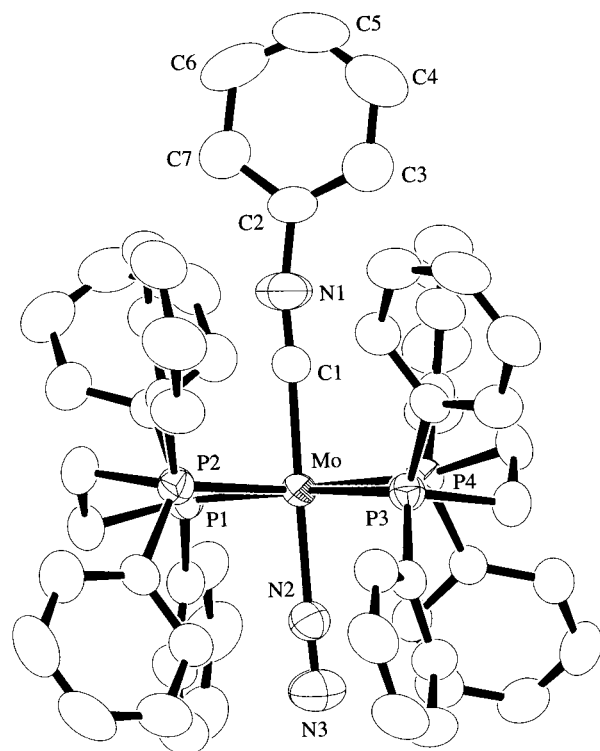


Figure 1. ORTEP diagram of **7a**. Hydrogen atoms are omitted for clarity.

Table 1. Selected Bond Lengths (Å) and Angles (deg) in **7a**

(a) Bond Length			
Mo–P(1)	2.4548(9)	Mo–P(2)	2.4491(9)
Mo–P(3)	2.4544(9)	Mo–P(4)	2.4481(9)
Mo–N(2)	2.102(3)	Mo–C(1)	1.992(3)
N(1)–C(1)	1.179(4)	N(1)–C(2)	1.388(4)
N(2)–N(3)	1.102(3)		
(b) Bond Angle			
P(1)–Mo–P(2)	79.91(3)	P(1)–Mo–P(3)	174.12(3)
P(1)–Mo–P(4)	102.74(3)	P(1)–Mo–N(2)	87.61(7)
P(1)–Mo–C(1)	89.90(9)	P(2)–Mo–P(3)	96.97(3)
P(2)–Mo–P(4)	172.62(3)	P(2)–Mo–N(2)	97.22(8)
P(2)–Mo–C(1)	86.71(9)	P(3)–Mo–P(4)	80.97(3)
P(3)–Mo–N(2)	87.86(7)	P(3)–Mo–C(1)	94.91(9)
P(4)–Mo–N(2)	89.80(8)	P(4)–Mo–C(1)	86.41(9)
N(2)–Mo–C(1)	174.9(1)	C(1)–N(1)–C(2)	167.4(4)
Mo–N(2)–N(3)	177.1(3)	Mo–C(1)–N(1)	176.7(3)

trans to the N_2 is CO ,^{6a} N_2 ,³ nitriles,²¹ or isocyanides coordinated to the $\text{Mo}(0)$ center in an end-on manner. Comparison of the IR data for these complexes provides the order of the $\nu(\text{NN})$ values decreasing as $\text{L} = \text{CO}$ (2128 cm^{-1}) > PhNC (2049 cm^{-1}) > N_2 (2020_{sym} , $1970_{\text{asym}}\text{ cm}^{-1}$) > $p\text{-MeOC}_6\text{H}_4\text{CN}$ (1946 cm^{-1}). Force constants calculated from these $\nu(\text{NN})$ values are 18.7, 17.3, 16.4, and 15.6 mdyn/Å , respectively.²² This indicates that the π -acidity of L decreases according to this order, which results in the increase in the net π -donating nature of the $\{\text{Mo}(\text{L})(\text{dppe})_2\}$ moiety toward the antibonding orbitals of the N_2 ligand.

(20) The X-ray analyses have also been undertaken for **7c**, **7f**, and **7g**. Although the refinements were not completed to the satisfactory level, the preliminary results have clearly demonstrated that the structures of these three complexes are essentially analogous to that of **7a**. See Experimental Section.

(21) Tatsumi, T.; Hidai, M.; Uchida, Y. *Inorg. Chem.* **1975**, *14*, 2530.

(22) (a) Lazarowich, N. J.; Morris, R. H.; Ressler, J. M. *Inorg. Chem.* **1986**, *25*, 3926. (b) Morris, R. H.; Earl, K. A.; Luck, R. L.; Lazarowich, N. J.; Sella, A. *Inorg. Chem.* **1987**, *26*, 2674, and references therein.

(19) (a) Wilkinson, P. G.; Houk, N. B. *J. Chem. Phys.* **1956**, *24*, 528. (b) Gordon, A. J.; Ford, R. A. *The Chemist's Companion*; John Wiley & Sons: New York, 1972; p 107.

The $\nu(\text{NN})$ value (2049 cm^{-1}) is considerably lower than that of free N_2 (2331 cm^{-1}) but still higher than the parent N_2 complex **1** (2020 and 1970 cm^{-1}).³ Thus, the N_2 ligand in **7a** is so labile as to be converted readily into the related $\text{Mo}(0)$ isocyanide complexes *trans*-[Mo(PhNC)(L)(dppe)₂] (L = CO (**9a**), *p*-MeOC₆H₄CN (**10a**), and BuⁿCN (**11**)).

Preparation and Characterization of *trans*-[Mo(RNC)(CO)(dppe)₂] (9**), *trans*-[Mo(RNC)(*p*-MeOC₆H₄CN)(dppe)₂] (**10**), and *trans*-[Mo(PhNC)(BuⁿCN)(dppe)₂] (**11**).** When **7a** suspended in THF was treated with CO at room temperature, an isocyanide–carbonyl complex **9a** was readily obtained in excellent yield. Although the reaction of **7f** with CO appears to proceed more slowly, **9f** (R = Buⁿ) was able to be isolated in satisfactory yield by treatment of a benzene solution of **7f** with CO at 50°C . Reactions of **7a** or **7f** with ca. 2 equiv of *p*-MeOC₆H₄CN in benzene at room temperature also resulted in the replacement of the N_2 ligand by the nitrile to give isocyanide–nitrile complexes **10** in high yields. Detailed structures of **9a** and **10a** have been determined by X-ray analyses as described below. On the other hand, the reaction of **7a** with an equimolar amount of BuⁿCN at room temperature gave **11**, which was characterized by the spectroscopic and microanalytical data. This finding indicates that **7** can serve as the versatile precursor for preparing a wide range of Mo complexes containing two different isocyanides *trans*-[Mo(RNC)(R'NC)(dppe)₂]. The reactions forming **9–11** are summarized in eq 2.

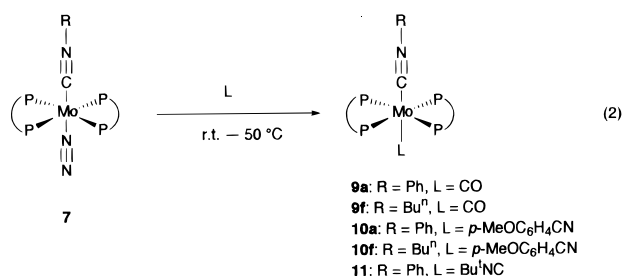


Table 2 lists the selected bond distances and angles in **9a** and **10a** determined by X-ray analyses. Since the attempt to prepare high-quality single crystals was unsuccessful for **11**, a single crystal of *trans*-[Mo(PhNC)₂(dppe)₂] (**12**)^{16a} was prepared and subjected to the X-ray diffraction study, whose results are also shown in Table 2. As depicted in Figures 2–4, structures of **9a**, **10a**, and **12**, respectively, are well comparable to that of **7a**, viz., the CO, *p*-MeOC₆H₄CN, and PhNC ligands occupy the *trans* position of the PhNC ligand in the octahedral coordination sphere. The Mo–C(8)–O, Mo–N(2)–C(8), and Mo–C(1)–N linkages in each complex are linear with angles of $177.9(4)^\circ$, $179.3(3)^\circ$, and $176.5(5)^\circ$, while the C(8)–O, N(2)–C(8), and C(1)–N bond distances in these moieties at $1.086(4)$, $1.153(4)$, and $1.171(6)\text{ \AA}$, respectively, are unexceptional for these molecules of this coordination mode.

For the PhNC ligands in *trans*-[Mo(PhNC)(L)(dppe)₂], important bonding parameters associated with **9a**, **10a**, and **12** are summarized in Table 3, together with those of **7a** for comparison. With respect to the bond lengths, Table 3 clearly shows that the C(1)–N(1) bonds are elongated, following the order **9a** < **12** < **7a** < **10a**, and

Table 2. Selected Bond Lengths (Å) and Angles (deg) in **9a, **10a**, and **12****

9a			
(a) Bond Length			
Mo–P(1)	2.429(1)	Mo–P(2)	2.439(1)
Mo–P(3)	2.434(1)	Mo–P(4)	2.422(1)
Mo–C(1)	2.072(4)	Mo–C(8)	2.017(5)
O–C(8)	1.086(4)	N(1)–C(1)	1.099(4)
N(1)–C(2)	1.407(5)		
(b) Bond Angle			
P(1)–Mo–P(2)	80.31(4)	P(1)–Mo–P(3)	176.10(4)
P(1)–Mo–P(4)	101.27(4)	P(1)–Mo–C(1)	86.4(1)
P(1)–Mo–C(8)	90.8(1)	P(2)–Mo–P(3)	98.34(4)
P(2)–Mo–P(4)	178.04(4)	P(2)–Mo–C(1)	91.4(1)
P(2)–Mo–C(8)	91.1(1)	P(3)–Mo–P(4)	80.16(4)
P(3)–Mo–C(1)	89.9(1)	P(3)–Mo–C(8)	92.9(1)
P(4)–Mo–C(1)	89.9(1)	P(4)–Mo–C(8)	87.7(1)
C(1)–Mo–C(8)	175.9(2)	C(1)–N(1)–C(2)	177.6(3)
Mo–C(1)–N(1)	179.2(4)	Mo–C(8)–O	177.9(4)
10a			
(a) Bond Length			
Mo–P(1)	2.464(1)	Mo–P(2)	2.457(1)
Mo–P(3)	2.414(1)	Mo–P(4)	2.432(1)
Mo–N(1)	2.160(3)	Mo–C(1)	1.964(3)
N(1)–C(1)	1.217(4)	N(1)–C(2)	1.386(4)
N(2)–C(8)	1.153(4)		
(b) Bond Angle			
P(1)–Mo–P(2)	80.09(4)	P(1)–Mo–P(3)	178.09(4)
P(1)–Mo–P(4)	99.14(4)	P(1)–Mo–N(2)	88.22(8)
P(1)–Mo–C(1)	97.9(1)	P(2)–Mo–P(3)	99.70(4)
P(2)–Mo–P(4)	177.24(4)	P(2)–Mo–N(2)	84.78(8)
P(2)–Mo–C(1)	98.0(1)	P(3)–Mo–P(4)	80.98(4)
P(3)–Mo–N(2)	89.88(8)	P(3)–Mo–C(1)	84.0(1)
P(4)–Mo–N(2)	92.56(8)	P(4)–Mo–C(1)	84.8(1)
N(2)–Mo–C(1)	173.6(1)	C(1)–N(1)–C(2)	149.8(4)
Mo–N(2)–C(8)	179.3(3)	Mo–C(1)–N(1)	168.9(3)
N(2)–C(8)–C(9)	173.4(4)		
12			
(a) Bond Length			
Mo–P(1)	2.461(2)	Mo–P(2)	2.445(2)
Mo–C(1)	2.031(6)	N–C(1)	1.171(6)
N–C(2)	1.399(7)		
(b) Bond Angle			
P(1)–Mo–P(1)*	101.90(8)	P(1)–Mo–P(2)	80.64(5)
P(1)–Mo–P(2)*	175.69(6)	P(1)–Mo–C(1)	88.9(2)
P(1)–Mo–C(1)*	89.4(2)	P(2)–Mo–P(2)*	97.04(8)
P(2)–Mo–C(1)	87.2(2)	P(2)–Mo–C(1)*	94.7(2)
C(1)–Mo–C(1)*	177.2(3)	C(1)–N–C(2)	172.7(7)
Mo–C(1)–N	176.5(5)		

accordingly the Mo–C(1) and N(1)–C(2) bond distances decrease as **9a** > **12** > **7a** > **10a**. This finding is interpreted in terms of the net π -donating ability of the {Mo(L)(dppe)₂} moieties toward the PhNC ligand, increasing in the order L = CO < PhNC < N₂ < *p*-MeOC₆H₄CN, which is in good agreement with the results obtained for a series of dinitrogen complexes *trans*-[Mo(N₂)(L)(dppe)₂] (vide supra). In contrast to relatively small differences in the bond angles of the Mo–C(1)–N(1) arrays ($179.2(4)$ – $168.9(3)^\circ$), those of the C(1)–N(1)–C(2) linkages change significantly, from $177.6(5)^\circ$ in **9a** to $149.8(4)^\circ$ in **10a**. In general, bent C–N–C linkages are found in the aliphatic isocyanides bound to the zerovalent metal center having no π -accepting ligands, where the electron density remains localized on the N atom in the NC group and the C–N–C linkage tends to be bent due to the pairing effects of electrons,²³ e.g., the average C–N–C angle of 130° for the two equatorial isocyanide ligands in the trigonal bipyramidal [Ru(CNBUⁿ)₄(PPh₃)] and that of

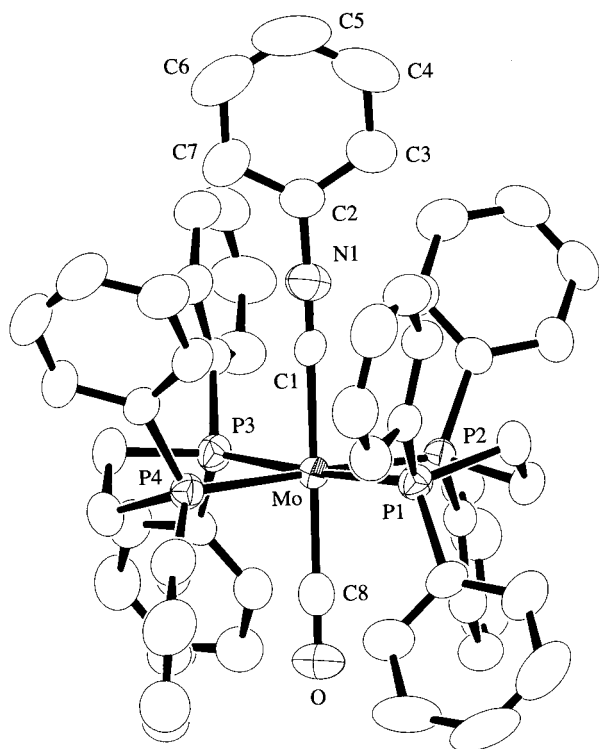


Figure 2. ORTEP diagram of **9a**. Hydrogen atoms are omitted for clarity.

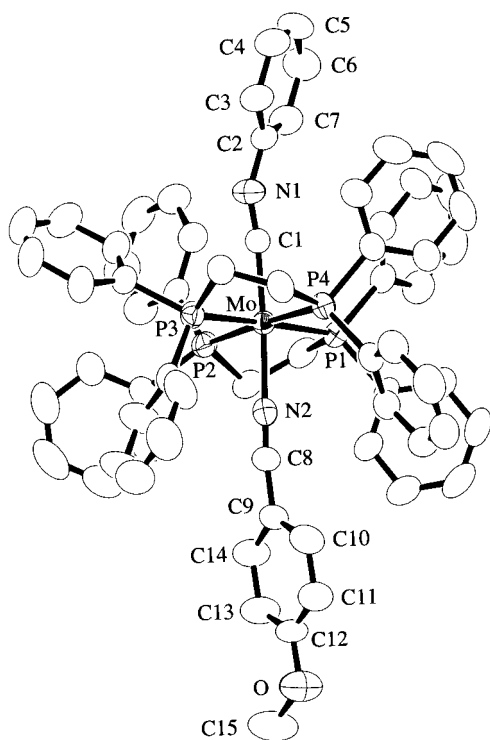


Figure 3. ORTEP diagram of **10a**. Hydrogen atoms are omitted for clarity.

135° for the two bent isocyanide ligands in $[\text{Fe}(\text{CN-Bu}^t)_5]$.²⁴ On the other hand, significant C–N–C bending hardly occurs for the aryl isocyanide ligands because of their ability to delocalize the charge from the isocyanide

(23) Hu, C.; Hodgeman, W. C.; Bennett, D. W. *Inorg. Chem.* **1996**, *35*, 1621.

(24) Basset, J.-M.; Berry, D. E.; Barker, G. K.; Green, M.; Howard, J. A. K.; Stone, F. G. A. *J. Chem. Soc., Dalton Trans.* **1979**, 1003.

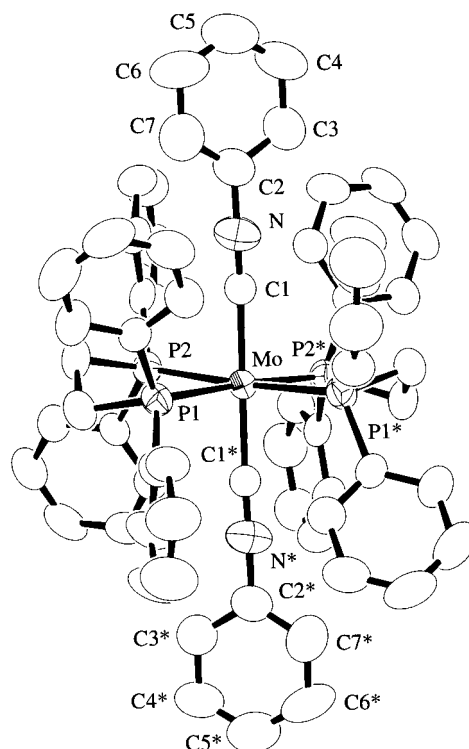


Figure 4. ORTEP diagram of **12**. Hydrogen atoms are omitted for clarity.

Table 3. Selected Bonding Parameters in $\text{trans-[Mo(PhNC)(L)(dppe)_2]}$

L	9a	12	7a	10a
	CO	PhNC	N ₂	<i>p</i> -MeOC ₆ H ₄ CN
(a) Bond Length (Å)				
Mo–C(1)	2.072(4)	2.031(6)	1.992(3)	1.964(3)
C(1)–N(1)	1.099(4)	1.171(6)	1.179(4)	1.217(4)
N(1)–C(2)	1.407(5)	1.399(7)	1.388(4)	1.386(4)
(b) Bond Angle (deg)				
Mo–C(1)–N(1)	179.2(4)	176.5(5)	176.7(3)	168.9(3)
C(1)–N(1)–C(2)	177.6(5)	172.7(7)	167.4(4)	149.8(4)

N atom into the aromatic rings; *cis*- $[\text{W}(\text{CNC}_6\text{H}_4\text{NC})_2(\text{dppe})_2]$ provides the rare example containing the bent aryl isocyanide ligands with C–N–C angles of 136.8(11)° and 141.4(8)°. This tendency is consistent with the finding that the C–N–C angle in *trans*- $[\text{Mo}(\text{PhNC})_2(\text{dppe})_2]$ (172.9(8)°) is larger than that in *trans*- $[\text{Mo}(\text{MeNC})_2(\text{dppe})_2]$ (156(1)°).²⁵ In this respect, the substantially bent C–N–C angle of 149.8(4)° observed in the PhNC complex **10a** is noteworthy.

All of the $^{31}\text{P}\{^1\text{H}\}$ NMR spectra for **9–11** show one singlet assignable to the dppe ligands, indicating that all have the *trans* structure, demonstrated by the X-ray analyses for **9a** and **10a**. In the IR spectra appear the intense bands characteristic of the C–O and C–N multiple bonds in the carbonyl, nitrile, and isocyanide ligands. Splitting of the $\nu(\text{NC})$ band in **9a** (2017 and 1991 cm^{-1}) might be explained by the packing effect as observed previously for **4** and its W analogue.^{6a,13} By using the $\nu(\text{NC})$ frequencies observed for a series of *trans*- $[\text{Mo}(\text{PhNC})(\text{L})(\text{dppe})_2]$, force constants of the isocyanide N–C multiple bonds may be calculated to be 15.3 (av), 14.4, 13.9, and 12.6 $\text{mdyn}/\text{\AA}$ for L = CO,

(25) Chatt, J.; Pombeiro, A. J. L.; Richards, R. L.; Royston, G. H. D.; Muir, K. W.; Walker, R. *J. Chem. Soc., Chem. Commun.* **1975**, 708.

PhNC, N₂, and *p*-MeOC₆H₄CN, respectively, and this order is similar to that observed for the force constants of the N–N bonds in *trans*-[Mo(N₂)(L)(dppe)₂] (vide supra).

Preparation and Characterization of *trans*-[Mo(RNC)(η^2 -H₂)(dppe)₂] (13). Activation of the H–H bond on transition metal centers is of much interest,²⁶ and the binding of H₂ to the 16e species [M(CO)(R₂-PCH₂CH₂PR₂)₂] (M = Mo, R = aryl, alkyl; M = W, R = aryl) and [Mn(CO)(R₂PCH₂CH₂PR₂)₂]⁺ (R = alkyl, aryl) has been investigated extensively. From these studies, several η^2 -H₂ complexes have already been isolated and characterized in a well-defined manner, which include *trans*-[Mo(CO)(η^2 -H₂)(R₂PCH₂CH₂PR₂)₂] (R = Ph,⁹ PhCH₂, *m*-CH₃C₆H₄CH₂²⁷) and *trans*-[Mn(CO)(η^2 -H₂)(R₂-PCH₂CH₂PR₂)₂]⁺ (R = Et, Ph).²⁸ In contrast, it has been revealed that the reactions of Mo complexes containing more electron-donating diphosphines under H₂ afford dihydride complexes [Mo(CO)H₂(R₂PCH₂CH₂PR₂)₂] (R = Et, Bu^t).^{9b,29} The analogous electronic control has been achieved by replacing the Mo atom with the more electron-rich W, which results in the formation of dihydride complex [W(CO)H₂(Ph₂PCH₂CH₂PPh₂)₂].¹³

Now the reactions of **7** containing a readily replaceable N₂ ligand with H₂ have been investigated to clarify the interaction of H₂ with the {Mo(RNC)(dppe)₂} chromophore. This will demonstrate for the first time the effect of the ligand occupying the site trans to the H₂ upon the bonding of the incorporated H₂. In contrast to the reactions with CO, nitriles, and isocyanides, initial attempts to prepare [Mo(RNC)(H₂)(dppe)₂] through the direct substitution of the N₂ ligand in **7** by H₂ (1 atm) at room temperature or 50 °C were unsuccessful, since most of **7** was recovered even after the prolonged reaction time. However, when a toluene solution of **7a** was heated at 90 °C for 30 min or a benzene solution of **7e** was refluxed for 30 min under Ar to dissociate the N₂ ligand and then the resultant black solutions presumably containing the five-coordinate complexes [Mo(RNC)(dppe)₂] (**8**) were treated with H₂ gas (1 atm), the desired H₂ complexes *trans*-[Mo(RNC)(η^2 -H₂)(Ph₂PCH₂CH₂PPh₂)₂] (**13a**, R = Ph; **13e**, R = *p*-Me₂NC₆H₄) could be isolated in moderate yields (Scheme 3).

Since the N₂ ligands in the isocyanide complexes **7** are bound to the Mo center more firmly than the N₂ in **4** containing the more electron-withdrawing CO ligand, removal of the N₂ to give the reactive five-coordinate species **8** probably requires more forcing conditions than those for generating **5** from **4**. This well correlates to the previous findings that **5** is readily obtained by bubbling Ar gas through a benzene solution of **4** at 50 °C for several minutes or degassing it in vacuo, whereas the W analogue [W(CO)(dppe)₂] (**14**) is isolable after refluxing a benzene solution of *trans*-[W(CO)(N₂)(dppe)₂] (**15**) under Ar, owing to the presence of the more

Scheme 3

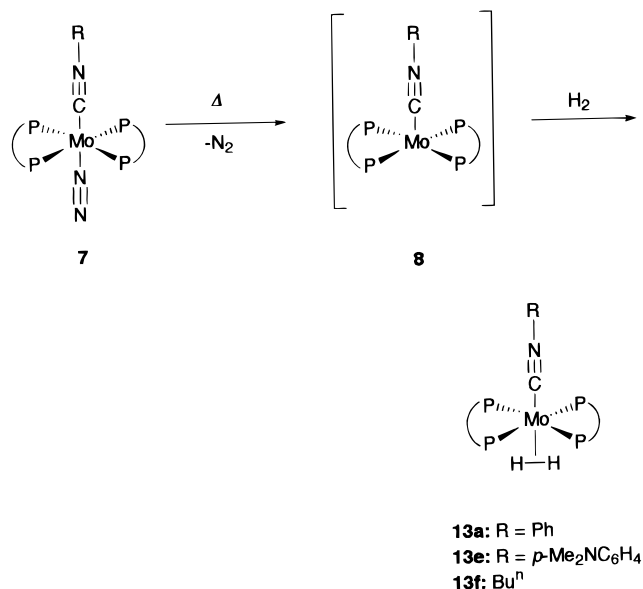


Table 4. *T*₁ Values for the H₂ Signal in *trans*-[Mo(CNR)(H₂)(dppe)₂] (**13**)^a

temp (K)	13a		13e		13f	
	δ	<i>T</i> ₁ (ms)	δ	<i>T</i> ₁ (ms)	δ	<i>T</i> ₁ (ms)
290	−4.8	<i>b</i>	−5.4	<i>b</i>	−5.9	20
260		21		15		15
230		17		20		17

^a 400 MHz; toluene-*d*₈ solutions. Inversion recovery method.
^b Data are unreliable due to much broadening of the signal.

electron-rich W center. The IR data of **4**, **15**, and **7** support this observation; the ν(NN) bands appear at 2110 and 2080 cm^{−1} for **4** and at 2070 and 2030 cm^{−1} for **15**, indicating the presence of the stronger back-donation to the N₂ ligand in **15**. The fact that the ν(NN) values observed for **7** are almost the same or lower than those of **15** is consistent with the requirement of the drastic conditions to generate **8**.

Despite the repeated trials, characterization of **8** could not be completed possibly due to its extreme sensitivity to air and moisture. Thus, although dark brown crystals obtained from the black solution produced after thermolysis of **7e** showed the satisfactory analytical data to be formulated as [Mo(*p*-Me₂NC₆H₄NC)(dppe)₂] (**8e**), reliable spectral data were unable to be collected. As observed for **5** and **14**, solutions possibly containing **8** were treated with N₂ to give **7** reversibly.

Taking into account the weaker π-acidity of the RNC ligands than the CO ligand, **13** had been expected to have dihydride ligands rather than a H₂ ligand. However, the ¹H NMR spectra for **13a** and **13e** both exhibited broad signals at −4.8 and −5.2 ppm, which are characteristic of the η^2 -H₂ protons. As summarized in Table 4, the *T*₁ values in the range 15–21 ms at 230 and 260 K are comparable to 20 ms at 200 K of the fully characterized dihydrogen complex *trans*-[Mo(CO)(η^2 -H₂)(dppe)₂] (**16**),⁹ indicating unambiguously that these can be identified as the η^2 -H₂ complexes.²⁶ Even for **13f** (R = Buⁿ), possibly having the more π-donating {Mo-(BuⁿNC)(dppe)₂} moiety, the η^2 -H₂ nature has been demonstrated by the NMR data at 230, 260, and 290 K as listed in Table 4, although isolation of the pure

(26) (a) Heinekey, D. M.; Oldham, W. J., Jr. *Chem. Rev.* **1993**, 93, 913. (b) Crabtree, R. H. *Angew. Chem., Int. Ed. Engl.* **1993**, 32, 789. (c) Jessop, P. G.; Morris, J. H. *Coord. Chem. Rev.* **1992**, 121, 155. (d) Kubas, G. J. *Acc. Chem. Res.* **1994**, 27, 183.

(27) Luo, X.-L.; Kubas, G. J.; Burns, C. J.; Eckert, J. *Inorg. Chem.* **1994**, 33, 5219.

(28) (a) King, W. A.; Scott, B. L.; Eckert, J.; Kubas, G. J. *Inorg. Chem.* **1999**, 38, 1069. (b) King, W. A.; Luo, X.-L.; Scott, B. L.; Kubas, G. J.; Zilm, K. W. *J. Am. Chem. Soc.* **1996**, 118, 6782.

(29) Kubas, G. J.; Ryan, R. R.; Unkefer, C. J. *J. Am. Chem. Soc.* **1987**, 109, 8113.

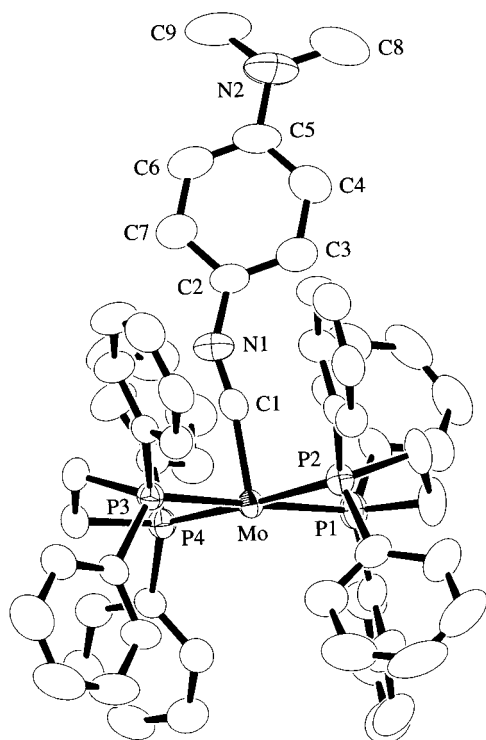


Figure 5. ORTEP diagram of **13e**. Hydrogen atoms are omitted for clarity.

Table 5. Selected Bond Lengths (Å) and Angles (deg) in **13e**

(a) Bond Length			
Mo-P(1)	2.454(1)	Mo-P(2)	2.443(1)
Mo-P(3)	2.410(1)	Mo-P(4)	2.431(1)
Mo-C(1)	1.969(4)	N(1)-C(1)	1.213(4)
N(1)-C(2)	1.385(4)		
(b) Bond Angle			
P(1)-Mo-P(2)	80.41(3)	P(1)-Mo-P(3)	179.22(4)
P(1)-Mo-P(4)	99.25(3)	P(1)-Mo-C(1)	96.82(10)
P(2)-Mo-P(3)	99.05(3)	P(2)-Mo-P(4)	177.84(4)
P(2)-Mo-C(1)	91.1(1)	P(3)-Mo-P(4)	81.27(3)
P(3)-Mo-C(1)	82.63(10)	P(4)-Mo-C(1)	86.8(1)
C(1)-N(1)-C(2)	148.4(4)	Mo-C(1)-N(1)	171.2(3)

compound showing satisfactory microanalysis data was unsuccessful.

The X-ray analysis was carried out for **13e**, whose results are shown in Figure 5 and Table 5. Although the η^2 -H₂ moiety could not be located, **13e** has a common octahedral structure and the η^2 -H₂ ligand is inferred to be present at the site trans to the isocyanide. The structure clarified here is well comparable to that of fully characterized **16**.⁹ By contrast, seven-coordinate dihydride complexes [W(CO)H₂(dppe)₂]¹³ and [Mo(CO)H₂(Et₂PCH₂CH₂PEt₂)₂]²⁹ tend to have a pentagonal bipyramidal geometry. Morris et al. claimed previously that treatment of the octahedral d⁶ N₂ complexes exhibiting a ν (NN) band in the region 2060–2150 cm⁻¹ with H₂ results in the formation of stable η^2 -H₂ complexes.^{30,31} It is noteworthy that **13a** and **13e** have apparently the well-characterized η^2 -H₂ ligand despite

the appearance of the ν (NN) band at 2048 and 2018 cm⁻¹ for **7a** and **7e**, respectively.

It is interesting that the C(1)–N(1) bond in the isocyanide ligand in **13e** is fairly long at 1.213(4) Å and the C(1)–N(1)–C(2) linkage is significantly bent with an angle of 148.4(4)°, which reflect the quite weak π -accepting nature of the η^2 -H₂ ligand in this complex. Considerably low ν (NC) frequencies observed for **13** (e.g., **13a**, 1875 and 1817; **13e**, 1891 and 1813 cm⁻¹) also arise from this electronic feature of the η^2 -H₂ ligand.

Experimental Section

General Considerations. All manipulations were carried out under an atmosphere of nitrogen except for those stated otherwise. IR and NMR spectra were recorded on JASCO FT/IR-420 and JEOL EX-270 or LA-400 spectrometers. The signals arising from the aromatic protons are omitted in the following ¹H NMR data. Elemental analyses were done with a Perkin-Elmer 2400 series II CHN analyzer. Amounts of solvating molecules in the crystals were determined by the X-ray crystallography, NMR measurement, and/or GLC analysis. Complexes **1**³² and **12**^{16a} were prepared according to the literature methods.

Preparation of *trans*-[Mo(RNC)(N₂)(dppe)₂] (7**) from Benzaldehyde Imines.** Preparation of **7a** (R = Ph). Complex **1** (166 mg, 0.175 mmol) and PhCH=NPh (33 mg, 0.18 mol) were dissolved in benzene (2 mL), and the solution was heated at reflux for 2 h. After cooling, ether was layered on the resulting dark red solution. Dark red crystals of **7a**·2C₆H₆ deposited, which were filtered off and dried in vacuo (129 mg, 62%). Anal. Calcd for C₇₁H₆₅N₃MoP₄: C, 72.26; H, 5.55; N, 3.56. Found: C, 71.99; H, 5.70; N, 3.23. IR (KBr): ν (NN), 2049; ν -(NC), 1910 cm⁻¹. ¹H NMR (C₆D₆): δ 2.35 (br, 8H, PCH₂). ³¹P-{¹H} NMR (C₆D₆): δ 68.9 (s).

Preparation of **7b (R = C₆H₄Me-*p*).** This compound was obtained from **1** (166 mg, 0.175 mmol) and PhCH=NC₆H₄Me-*p* (68 mg, 0.35 mmol) by essentially the same procedure as that for preparing **7a** except that the red crystals of **7b**·C₆H₆ were isolated by addition of hexane to the product solution. Yield: 52%. Anal. Calcd for C₆₆H₆₁N₃MoP₄: C, 71.03; H, 5.51; N, 3.77. Found: C, 71.02; H, 5.73; N, 3.23. IR (KBr): ν (NN), 2053; ν -(NC), 1914 cm⁻¹. ¹H NMR (C₆D₆): δ 2.11 (s, 3H, Me), 2.40 (br, 8H, PCH₂). ³¹P-{¹H} NMR (C₆D₆): δ 69.1 (s).

The following compounds **7c–7g** were obtained similarly, except that **1** (0.175 mmol) was reacted with a larger excess of the imine (1.75 mmol).

7c·3/2C₆H₆ (R = C₆H₄OMe-*p*): Red crystals, yield 46%. Anal. Calcd for C₆₉H₆₄N₃MoP₄: C, 70.77; H, 5.51; N, 3.59. Found: C, 70.12; H, 5.74; N, 3.11. IR (KBr): ν (NN), 2054; ν -(NC), 1908 cm⁻¹. ¹H NMR (C₆D₆): δ 3.31 (s, 3H, OMe), 2.41 (br, 8H, PCH₂). ³¹P-{¹H} NMR (C₆D₆): δ 69.0 (s). Repeated purification did not improve the analysis data.

7d·1/2C₆H₆ (R = C₆H₄F-*p*): Orange crystals, yield 35%. Anal. Calcd for C₆₂H₅₅N₃FMoP₄: C, 68.89; H, 5.13; N, 3.89. Found: C, 68.23; H, 5.43; N, 3.58. IR (KBr): ν (NN), 2054; ν -(NC), 1907 cm⁻¹. ¹H NMR (C₆D₆): δ 2.3–2.5 (m, 8H, PCH₂). ³¹P-{¹H} NMR (C₆D₆): δ 68.7 (s). Repeated purification did not result in the better carbon analysis.

7e (R = C₆H₄NMe₂-*p*): Orange crystals, yield 38%. Anal. Calcd for C₆₁H₅₈N₄MoP₄: C, 68.67; H, 5.48; N, 5.25. Found: C, 68.70; H, 5.68; N, 5.22. IR (KBr): ν (NN), 2018; ν (NC), 1929 cm⁻¹. ¹H NMR (C₆D₆): δ 2.51 (s, 6H, NMe), 2.41 (br, 8H, PCH₂). ³¹P-{¹H} NMR (C₆D₆): δ 69.1 (s).

7f (R = Buⁿ): Orange crystals, yield 56%. Anal. Calcd for C₅₇H₅₇N₃MoP₄: C, 68.19; H, 5.72; N, 4.19. Found: C, 68.63; H, 5.60; N, 4.02. IR (KBr): ν (NN) and ν (NC), 1964 cm⁻¹. ¹H

(30) Morris, R. H.; Earl, K. A.; Luck, R. L.; Lazarowich, N. J.; Sella, A. *Inorg. Chem.* **1987**, *26*, 2674.

(31) In the IR spectrum of **7f**, a very strong and broad band centered at 1963 cm⁻¹ appeared. The NN and NC stretching bands are probably overlapping, and it was impossible to assign the correct ν (NN) frequency.

(32) Hussain, W.; Leigh, G. J.; Mohd.-Ali, H.; Pickett, C. J.; Rankin, D. A. *J. Chem. Soc., Dalton Trans.* **1984**, 1703.

NMR (C_6D_6): δ 0.83 (t, J = 7.1 Hz, 3H, CH_2Me), 1.0–1.2 (m, 4H, CH_2CH_2Me), 2.90 (t, J = 6.5 Hz, 2H, NCH_2), 2.2–2.5 (br m, 8H, PCH_2). $^{31}P\{^1H\}$ NMR (C_6D_6): δ 70.0 (s).

7g (**R** = **Pr**¹): Orange-red crystals, yield 60%. Anal. Calcd for $C_{56}H_{55}N_3MoP_4$: C, 67.95; H, 5.60; N, 4.24. Found: C, 67.80; H, 5.61; N, 3.96. IR (KBr): $\nu(NN)$, 2035; $\nu(NC)$, 1929 cm^{-1} . 1H NMR (C_6D_6): δ 0.67 (d, J = 6.4 Hz, 6H, Me), 3.37 (sep, J = 6.4 Hz, 1H, NCH), 2.3–2.5 (m, 8H, PCH_2). $^{31}P\{^1H\}$ NMR (C_6D_6): δ 70.0 (s).

7h· C_6H_6 (**R** = **CH₂Ph**). A mixture of **1** (167 mg, 0.176 mmol) and $PhCH=NCH_2Ph$ (166 μ L, 0.882 mmol) in benzene (3 mL) was refluxed for 5 min, and the resultant dark green solution was filtered. Addition of hexane (10 mL) to the filtrate gave orange-red crystals of **7h**· C_6H_6 (111 mg, 56%). Anal. Calcd for $C_{66}H_{61}N_3MoP_4$: C, 71.03; H, 5.51; N, 3.77. Found: C, 70.75; H, 5.47; N, 3.68. IR (KBr): $\nu(NN)$, 1972; $\nu(NC)$, 1933 cm^{-1} . 1H NMR (C_6D_6): δ 4.13 (s, 2H, NCH_2), 2.3–2.5 (m, 8H, PCH_2). $^{31}P\{^1H\}$ NMR (C_6D_6): δ 69.9 (s).

Quantitative Analysis of the Benzene Produced in the Reaction Forming 7. A mixture of **1** (104 mg, 0.110 mmol) and $PhCH=NPh$ (22.7 mg, 0.125 mmol) in toluene (1 mL) was refluxed under N_2 for 1 h. After cooling to room temperature, the resultant solution was subjected to the GLC analysis using a Shimadzu GC-14A Gas Chromatograph equipped with a 25 m \times 0.25 mm fused silica capillary column, which showed the formation of 0.71 mol of benzene per Mo atom. Formation of benzene (0.73 mol/Mo atom) from the reaction of **1** with $PhCH=NC_6H_4Me-p$ in *p*-xylene was confirmed by the analogous method.

Preparation of *trans*-[Mo(PhNC)(CO)(dppe)₂] (9a). Through a suspension of **7a**· $2C_6H_6$ (114 mg, 0.0966 mmol) in THF (5 mL) was passed CO gas for a few minutes, and the mixture was stirred under CO for 25 h at room temperature. The resultant orange solid was filtered off, washed with THF and ether, and then dried in vacuo (57 mg, 58%). Addition of hexane (10 mL) to the combined THF filtrate afforded the second crop of **9a** as orange prisms (18 mg, 18%). Anal. Calcd for $C_{60}H_{53}NMoOP_4$: C, 70.38; H, 5.22; N, 1.37. Found: C, 69.88; H, 5.19; N, 1.53. IR (KBr): $\nu(NC)$, 2017 and 1991; $\nu(CO)$, 1812 cm^{-1} . 1H NMR (C_6D_6): δ 2.35 (br, 8H, PCH_2). $^{31}P\{^1H\}$ NMR (C_6D_6): δ 72.1 (s).

Preparation of *trans*-[Mo(BuⁿNC)(CO)(dppe)₂] (9f). A benzene solution (15 mL) of **7f** (307 mg, 0.306 mmol) was stirred under CO at 50 °C for 3 h, and the resulting orange mixture was filtered. Hexane was added to the concentrated filtrate, affording **9f** as orange crystals (190 mg, 62% yield). Anal. Calcd for $C_{58}H_{57}NMoOP_4$: C, 69.39; H, 5.72; N, 1.40. Found: C, 68.75; H, 5.69; N, 1.66. IR (KBr): $\nu(NC)$, 2075; $\nu(CO)$, 1788 cm^{-1} . 1H NMR (C_6D_6): δ 0.71 (t, J = 6.4 Hz, 3H, Me), 0.8–0.9 (m, 4H, $MeCH_2CH_2$), 2.40 (m, 2H, NCH_2), 2.2–2.3 (m, 8H, PCH_2). $^{31}P\{^1H\}$ NMR (C_6D_6): δ 73.4 (s).

Preparation of *trans*-[Mo(PhNC)(*p*-MeOC₆H₄CN)(dppe)₂] (10a). A mixture of **7a**· $2C_6H_6$ (315 mg, 0.308 mmol) and *p*-MeOC₆H₄CN (78 mg, 0.59 mmol) in benzene (17 mL) was stirred at room temperature for 24 h. Addition of hexane to the resultant solution gave dark brown prisms of **10a**· $1/2C_6H_6$ (290 mg, 84% yield). Anal. Calcd for $C_{70}H_{63}N_2MoOP_4$: C, 71.98; H, 5.44; N, 2.40. Found: C, 71.93; H, 5.27; N, 2.24. IR (KBr): $\nu(CN_{nitrile})$, 2171; $\nu(NC_{isocyanide})$, 1821 and 1715 cm^{-1} . 1H NMR (C_6D_6): δ 3.13 (s, 3H, OMe), 2.3–2.7 (m, 8H, PCH_2). $^{31}P\{^1H\}$ NMR (C_6D_6): δ 70.2 (s).

Preparation of *trans*-[Mo(BuⁿNC)(*p*-MeOC₆H₄CN)(dppe)₂] (10f). This complex was obtained similarly from **7f** and *p*-MeOC₆H₄CN as dark brown crystals in 78% yield. Anal. Calcd for $C_{65}H_{64}N_2MoOP_4$: C, 70.39; H, 5.82; N, 2.53. Found: C, 70.27; H, 5.85; N, 2.58. IR (KBr): $\nu(CN_{nitrile})$, 2154; $\nu(NC_{isocyanide})$, 1734 cm^{-1} . 1H NMR (C_6D_6): δ 0.93 (t, J = 7.4 Hz, 3H, CH_2Me), 1.26 and 1.40 (m, 2H each, $NCH_2CH_2CH_2$), 3.22 (t, J = 6.6 Hz, 2H, NCH_2), 3.10 (s, 3H, OMe), 2.35–2.55 (m, 8H, PCH_2). $^{31}P\{^1H\}$ NMR (C_6D_6): δ 71.8 (s).

Preparation of *trans*-[Mo(PhNC)(BuⁿNC)(dppe)₂] (11). A mixture of **7a**· $2C_6H_6$ (99 mg, 0.097 mmol) and BuⁿNC (11 μ L, 0.098 mmol) in benzene (5 mL) was stirred at room temperature for 24 h. Crystallization from benzene/hexane afforded **11**· C_6H_6 (57 mg, 51% yield) as dark brown crystals. Anal. Calcd for $C_{70}H_{68}N_2MoP_4$: C, 72.66; H, 5.92; N, 2.42. Found: C, 72.50; H, 5.87; N, 2.60. IR (KBr): $\nu(NC)$, 2010 (Buⁿ-NC) and 1880 (PhNC) cm^{-1} . 1H NMR (C_6D_6): δ 0.64 (s, 9H, Buⁿ), 2.2–2.5 (m, 8H, PCH_2). $^{31}P\{^1H\}$ NMR (C_6D_6): δ 73.3 (s).

Preparation of [Mo(*p*-Me₂NC₆H₄CN)(dppe)₂] (8e). A benzene solution (5 mL) of **7e** (108 mg, 0.101 mmol) was refluxed under Ar for 40 min to give a yellow-black solution. After cooling to room temperature, hexane (10 mL) was added and the mixture was filtered. Addition of hexane (12 mL) to the concentrated filtrate (ca. 5 mL) afforded **8e** as dark brown crystals (40 mg, 38% yield), which were separated manually from undesired byproducts deposited as orange crystals. Anal. Calcd for $C_{61}H_{58}N_2MoP_4$: C, 70.52; H, 5.63; N, 2.70. Found: C, 70.38; H, 5.85; N, 2.89.

Preparation of *trans*-[Mo(PhNC)(η^2 -H₂)(dppe)₂] (13a). A toluene solution (4.5 mL) of **7a**· $2C_6H_6$ (99 mg, 0.097 mmol) was heated at 90 °C under Ar for 30 min. After cooling, the resultant yellowish black solution was degassed and then kept under H₂ (1 atm). The solution gradually turned to orange-red, from which red crystals of **13a**· $C_6H_5CH_3$ precipitated (46 mg, 43% yield). Addition of hexane to the filtrate gave the second crop (26 mg, 25% yield). Anal. Calcd for $C_{66}H_{63}NMoP_4$: C, 72.72; H, 5.83; N, 1.28. Found: C, 72.32; H, 5.74; N, 1.58. IR (KBr): $\nu(NC)$, 1875 and 1817 cm^{-1} . 1H NMR (C_6D_6): δ -4.8 (br, 2H, H₂), 2.15 (s, 3H, $C_6H_5CH_3$), 2.2–2.4 (m, 8H, PCH_2). $^{31}P\{^1H\}$ NMR (C_6D_6): δ 74.5 (s).

Preparation of *trans*-[Mo(*p*-Me₂NC₆H₄CN)(η^2 -H₂)(dppe)₂] (13e). A benzene solution (3 mL) of **7e** (84 mg, 0.078 mmol) was refluxed under Ar for 30 min. Analogous treatment of the resultant solution with H₂ afforded **13e**, which was obtained as orange-red crystals by recrystallization from benzene–hexane (60 mg, 74% yield). Anal. Calcd for $C_{61}H_{60}N_2MoP_4$: C, 70.38; H, 5.81; N, 2.69. Found: C, 70.01; H, 5.86; N, 2.67. IR (KBr): $\nu(NC)$, 1891 and 1813 cm^{-1} . 1H NMR (C_6D_6): δ -5.2 (br, 2H, H₂), 2.55 (s, 6H, NCH_3), 2.3–2.6 (m, 8H, PCH_2). $^{31}P\{^1H\}$ NMR (C_6D_6): δ 75.1 (s).

Preparation of *trans*-[Mo(BuⁿNC)(η^2 -H₂)(dppe)₂] (13f). This complex was obtained from **7f** by the same procedure as that for **13e**. However, the compound is always contaminated by a small amount of byproduct(s), and satisfactory analysis data were not available. Anal. Calcd for $C_{57}H_{59}NMoP_4$: C, 70.01; H, 6.08; N, 1.43. Found: C, 69.27; H, 5.90; N, 1.61. IR (KBr): $\nu(NC)$, 1800–1900 cm^{-1} (vbr). 1H NMR (C_6D_6): δ -5.9 (br, 2H, H₂), 0.86 (t, J = 7.4 Hz, 3H, CH_3), 1.0–1.2 (m, 2H each, $NCH_2CH_2CH_2$), 2.94 (t, J = 6.6 Hz, 2H, NCH_2), 2.2–2.3 (m, 8H, PCH_2). $^{31}P\{^1H\}$ NMR (C_6D_6): δ 76.3 (s).

X-ray Diffraction Studies. Single crystals were sealed in glass capillaries under N_2 for **7a**, **9a**, **10a**, and **12** or under Ar for **13e**, which were transferred to a Rigaku AFC7R diffractometer equipped with a graphite-monochromatized Mo K α source. Diffraction studies were carried out at room temperature. Orientation matrixes and unit cell parameters were determined by least-squares treatment of 25 reflections with $35^\circ < 2\theta < 40^\circ$. The intensities of three check reflections were monitored every 150 reflections during data collection, which revealed no significant decay for all crystals. Intensity data were corrected for Lorentz and polarization effects and for absorption (ψ scans). Details of crystal and data collection parameters are summarized in Table 6.

Structure solution and refinements were carried out by using the teXsan program package.³³ The positions of the non-hydrogen atoms were determined by Patterson methods and

(33) teXsan: Crystal Structure Analysis Package; Molecular Structure Corp.: The Woodlands, TX, 1985 and 1992.

Table 6. Crystallographic Data for 7a·2C₆H₆, 12·C₆H₆, 9a, 10a·1/2C₆H₆, and 13e

	7a·2C ₆ H ₆	12·C ₆ H ₆	9a	10a·1/2C ₆ H ₆	13e
formula	C ₇₁ H ₆₅ N ₃ P ₄ Mo	C ₇₂ H ₆₄ N ₂ P ₄ Mo	C ₆₀ H ₅₃ NOP ₄ Mo	C ₇₀ H ₆₃ N ₂ OP ₄ Mo	C ₆₁ H ₆₀ N ₂ P ₄ Mo
fw	1180.15	1177.15	1023.92	1168.12	1040.99
space group	<i>P</i> $\bar{1}$ (No. 2)	<i>P</i> 2 ₁ / <i>c</i> (No. 13)	<i>P</i> 2 ₁ / <i>n</i> (No. 14)	<i>P</i> $\bar{1}$ (No. 2)	<i>P</i> $\bar{1}$ (No. 2)
<i>a</i> (Å)	11.3451(6)	12.233(2)	11.094(8)	10.382(2)	11.8428(8)
<i>b</i> (Å)	15.713(2)	12.391(5)	26.412(6)	12.113(2)	13.390(1)
<i>c</i> (Å)	17.645(2)	19.718(3)	17.392(5)	24.231(4)	18.522(1)
α (deg)	97.286(9)	90	90	100.70(1)	79.707(7)
β (deg)	93.183(6)	93.41(1)	100.16(3)	93.65(2)	81.434(6)
γ (deg)	103.892(7)	90	90	102.17(1)	65.707(6)
<i>V</i> (Å ³)	3016.6(5)	2983(1)	5016(3)	2909.9(9)	2624.7(4)
<i>Z</i>	2	2	4	2	2
ρ_{calc} (g cm ⁻³)	1.299	1.310	1.356	1.333	1.317
<i>F</i> (000)	1228	1224	2120	1214	1084
μ_{calc} (cm ⁻¹)	3.68	3.71	4.31	3.81	4.12
transmn factor	0.9091–0.9987	0.9218–0.9981	0.9709–0.9988	0.8559–0.0990	0.9541–0.9999
cryst size (mm ³)	0.4 × 0.4 × 0.2	0.2 × 0.2 × 0.2	0.5 × 0.15 × 0.1	0.7 × 0.7 × 0.15	0.8 × 0.5 × 0.3
scan type	ω –2 θ	ω –2 θ	ω	ω –2 θ	ω –2 θ
2 θ range (deg)	5–50	5–40	5–55	5–50	5–55
no. measd	11055	3150	12090	10809	12580
no. unique	10635	2973	11504	10280	12065
no. obsd	7090	2019	6280	7044	7352
no. var	713	357	605	703	846
<i>R</i> ^a	0.034	0.036	0.041	0.037	0.037
<i>R</i> _w ^b	0.033	0.036	0.036	0.036	0.038
GOF	1.41	1.53	1.35	1.62	1.66
residual peaks (e/Å ⁻³)	0.22, –0.23	0.36, –0.31	0.37, –0.40	0.52, –0.43	0.85, –0.33

^a $R = \sum ||F_o| - |F_c|| / \sum |F_o|$. ^b $R_w = [\sum w(|F_o| - |F_c|)^2 / \sum wF_o^2]^{1/2}$.

subsequent Fourier syntheses (DIRDIF PATTY),³⁴ which were refined anisotropically by full-matrix least-squares techniques. The hydrogen atoms in **13e** were found in the Fourier map except for the η^2 -H₂ hydrogens and refined isotropically, while unobserved η^2 -H₂ hydrogens were not included for refinements. For the other complexes, all hydrogen atoms were placed at the calculated positions and included in the final stages of refinements with fixed parameters.

X-ray diffraction studies were undertaken also for the following compounds. Although the analyses could not be completed as described below, the preliminary results clarified the atom connecting scheme in these compounds.

7c·3/2C₆H₆: *a* = 13.278(3) Å, *b* = 22.298(3) Å, *c* = 11.497(2) Å, α = 92.34(1)°, β = 113.43(1)°, and γ = 104.19(1)° with *Z* = 2 in space group *P* $\bar{1}$ (No. 2). *R* (*R*_w) = 0.067 (0.053) for 3594 data with *I* > 3.0 σ (*I*). Carbon atoms in the dppe ligands were treated only isotropically.

7f: *a* = 10.905(3) Å, *b* = 12.370(5) Å, *c* = 18.996(5) Å, α = 98.69(3)°, β = 101.42(2)°, and γ = 94.78(3)° with *Z* = 2 in space

group *P* $\bar{1}$ (No. 2). *R* (*R*_w) = 0.080 (0.082) for 3747 data with *I* > 3.0 σ (*I*). An uncharacterizable large peak still remained in the final Fourier map.

7g: *a* = 12.821(4) Å, *b* = 17.594(3) Å, *c* = 11.471(3) Å, α = 100.56(2)°, β = 103.47(3)°, and γ = 84.54(2)° with *Z* = 2 in space group *P* $\bar{1}$ (No. 2). *R* (*R*_w) = 0.078 (0.070) for 4825 data with *I* > 3.0 σ (*I*). The least-squares refinements resulted in the unusually large temperature factors for the Prⁱ carbons probably due to the disorder of this group.

Acknowledgment. This work was supported by the Ministry of Education, Science, Sports, and Culture of Japan (Grant Nos. 09102004 and 09238103).

Supporting Information Available: Tables of atomic coordinates and equivalent isotropic thermal parameters, anisotropic thermal parameters, and extensive bond lengths and angles, together with figures with full atom-numbering scheme, for **7a**, **9a**, **10a**, **12**, and **13e**. This material is available free of charge via the Internet at <http://pubs.acs.org>.

OM9904605

(34) PATTY: Beurskens, P. T.; Admiraal, G.; Beurskens, G.; Bosman, W. P.; Garcia-Granda, S.; Gould, R. O.; Smits, J. M. M.; Smykalla, C. *The DIRDIF program system*; Technical Report of the Crystallography Laboratory: University of Nijmegen, The Netherlands, 1992.